# Kieserite Solubility in the Aqueous $FeCl_3 + MgCl_2 + HCl$ System between (338 and 378) K

**Matthew W. Jones,[†] Vladimiros G. Papangelakis,*[,†] and Johann D. T. Steyl[‡]**

Department of Chemical Engineering and Applied Chemistry, University of Toronto, Wallberg Building, 200 College Street, Toronto, Ontario M5S 3E5, Canada, and Anglo Research, 8 Schonland Street, Theta, Johannesburg, South Africa

Kieserite ($MgSO_4 \cdot H_2O$) solubility was measured at temperatures between (338 and 378) K, $FeCl_3$ concentrations of 1.0 mol·kg$^{-1}$, $MgCl_2$ concentrations between (1.1 and 3) mol·kg$^{-1}$, and HCl concentrations between (0.5 and 2.3) mol·kg$^{-1}$. These conditions are of interest because of their relevance for processes designed to extract nickel from oxide ores by atmospheric leaching in mixed sulfate−chloride solutions. Experimental data were compared with model predictions generated by use of OLI Software's mixed solvent electrolyte (MSE) model. Model predictions for $MgSO_4 \cdot H_2O$ solubility were found to match experimental results with an average absolute deviation of ± 0.09 mol·kg$^{-1}$ and an average absolute relative deviation of 11.1 %. The ability of the model to accurately predict solubility trends in solutions not used in the development of model parameters validates the model.

## Introduction

The nickel industry is rapidly growing, and many new ore deposits to be used for nickel production are comprised of lateritic ores. In fact, more than half (72 %) of the nickel present in the Earth's crust exists in laterite form. However, only approximately 42 % of nickel produced comes from these sources.[1,2] In order to continue increasing nickel production to meet the ever-increasing world demand, laterite ores will need to be processed.

The majority of the world's laterite ore fields were formed in tropical regions, where high temperatures and a humid atmosphere lead to the weathering process that creates the various horizons of a laterite ore body. Over thousands of years, magnesium and silica have been leached and seep further below the surface, leaving an upper limonite layer consisting primarily of goethite. This upper layer generally consists of between (1 and 2) % Ni and can be used in production via high-pressure acid leaching (HPAL)[3] or the Caron process.[4] Beneath the limonite layer there is another layer consisting of magnesium-bearing silicate minerals known as the saprolite layer. This level is usually relatively high, that is (1.5 to 10) % in nickel, and can be refined economically by pyrometallurgical means.[5] The variable chemical nature of these ores makes it difficult to create a process capable of refining the whole ore body including these two ores and possible intermediate zones. However, one such process currently under development is the Anglo Research Nickel (ARNi) process, which also aims at refining so-called dry laterites.[6,7]

The reason the economics of hydrometallurgical processing of laterite ore are sensitive to high magnesium content is related to acid consumption.[8] Thus, in order for such a process to be economically feasible, the acid consumed must be regenerated and recycled at a cheaper rate as compared to the purchasing of the raw reagents. In addition, for a laterite leaching process to operate in a closed-circuit manner, it must be able to maintain its mass balance by rejecting magnesium. However, the high solubility of magnesium makes it difficult to economically remove from the system.

In chloride leach solutions, one possible method of magnesium removal is via pyrohydrolysis of a bleed solution stream. Pyrohydrolysis involves a reaction between $MgCl_2$ and water to form HCl and MgO.[9] Although the pyrohydrolysis reaction itself is relatively efficient, excess solution water needs to be coevaporated, which makes this process option very energy-intensive. The ARNi process involves a much less energy-intensive step in the primary circuit, during which simultaneous Mg removal and acid regeneration occur by purely chemical means, entitled the acid regeneration step. In this acid regeneration step, magnesium is precipitated as $MgSO_4 \cdot H_2O$ from a high strength chloride stream.

The main input to this step is a recycle stream that has had the majority of the dissolved iron and value metals removed previously. This stream contains high levels of $MgCl_2$, moderate levels of $FeCl_3$, and HCl and is combined with concentrated $H_2SO_4$. Because $MgSO_4$ is much less soluble than $MgCl_2$, the addition of $H_2SO_4$ at the boiling point results in the highest precipitation of the natural mineral kieserite by the following reaction:

$$MgCl_2 + H_2SO_4 + H_2O \leftrightarrow MgSO_4 \cdot H_2O(s) + 2HCl \quad (1)$$

$MgSO_4 \cdot H_2O$ solubility in the $MgSO_4/MgCl_2/FeCl_3/HCl/H_2O$ system is relatively low. However, the presence of $MgCl_2$ further reduces the solubility of $MgSO_4$ through the common ion effect with magnesium. In addition, the high chloride concentration will suppress $MgSO_4$ solubility through a salting-out effect. There are two important benefits to rejecting magnesium through reaction 1.

One of these advantages is that the high concentration of chloride ions ensures that kieserite, as opposed to $MgSO_4 \cdot 7H_2O$ (epsomite) or $MgSO_4 \cdot 6H_2O$ (hexahydrite), is the solid phase precipitated. The higher the hydration state of the $MgSO_4$ solids,

* Corresponding author. E-mail: vladimiros.papangelakis@utoronto.ca.
[†] University of Toronto.
[‡] Anglo Research.

10.1021/je800735h CCC: $40.75 
Published on Web 04/27/2009

the more energy would be required to convert the salt to MgO, the form in which magnesium may ultimately be rejected.

The other important advantage of this reaction is that it regenerates HCl. Since $H_2SO_4$ is less expensive than HCl, this is an efficient method of maintaining the acid level in a predominantly chloride stream without purchasing expensive HCl.[6,7] In this work the solubility of $MgSO_4 \cdot H_2O$ under conditions similar to those proposed for the acid regeneration stage of the ARNi process was studied.

To perform this task, experimental $MgCl_2 \cdot 6H_2O$ (bischofite) solubility data were generated in aqueous solutions containing $FeCl_3$ and HCl in order to gain insight into the ionic interactions between ferric chloride complexes and $Mg^{2+}$ ions in pure chloride solutions. These data were used to calibrate a model that had been created previously by use of OLI Software's mixed solvent electrolyte (MSE) model.[10] Once the model was completed, experimental $MgSO_4 \cdot H_2O$ solubility data were generated at relevant conditions and used to validate the developed model.

## Theoretical Section

***Equilibrium Constants.*** In order to calculate equilibrium constants by use of OLI's MSE model, thermodynamic parameters such as chemical potential, partial molar enthalpy, entropy, specific volume, and heat capacity are found in literature sources and input into the model database. These values are extended over a wide range of temperatures and pressures by use of the Helgeson−Kirkham−Flowers (HKF) equation of state model. Details of the HKF model can be seen in Tanger and Helgeson.[11] This model has been shown to be accurate at temperatures up to 1273 K and pressures up to 500 MPa.

***Activity Coefficient Model.*** The value of any model is derived from its ability to accurately predict conditions outside those used for the generation of its parameters. OLI System's MSE model combines fundamental thermodynamic equations with an empirical term to provide a means of calculating activity coefficients that is grounded in theory, but it can be adjusted to fit calculated equilibrium conditions to those seen experimentally. This is done by combining three terms for the excess Gibbs energy, $G^{EX}$:

$$\frac{G^{EX}}{RT} = \frac{G^{EX}_{LR}}{RT} + \frac{G^{EX}_{MR}}{RT} + \frac{G^{EX}_{SR}}{RT} \quad (2)$$

The long-range term $G^{EX}_{LR}$ is calculated by the Pitzer−Debye−Hückel equation, the short-range term $G^{EX}_{SR}$ is calculated by the UNIQUAC equation, and the middle-range term $G^{EX}_{MR}$ is calculated by an empirical second-order virial-type equation. The parameters for this term are adjusted for each pair of solution species, as the model's calculations are altered to match experimental results. The primary underlying assumption behind this model is that interaction parameters between species are independent of the composition of the surrounding solution. Thus, once a set of interaction parameters has been created for a species pair, it describes that interaction in any solution, regardless of what other species are present. The equation for the midrange activity coefficient term is shown here:

$$\ln \gamma_i^{MR} = \sum_i \sum_j x_i x_j B_{ij}(I_x) - \left(\sum_i n\right) \sum_i \sum_j x_i x_j \frac{\delta B_{ij}(I_x)}{\delta n_k} - 2\sum_i x_i B_{ik}(I_x) \quad (3)$$

where $x$ is the species mole fraction, $B_{ij}$ is the binary interaction parameter for species pair $i-j$, and $I_x$ is the ionic strength. The relationship of the $B_{ij}$ term to ionic strength is given by

$$B_{ij} = b_{ij} + c_{ij} \exp(-\sqrt{I_x + 0.01}) \quad (4)$$

where the $b_{ij}$ and $c_{ij}$ terms are the adjustable interaction parameters given by

$$b_{ij} = b_{ij,0} + b_{ij,1}T + \frac{b_{ij,2}}{T} \quad \text{and} \quad c_{ij} = c_{ij,0} + c_{ij,1}T + \frac{c_{ij,2}}{T} \quad (5)$$

These equations give the middle-range interaction term for both concentration and temperature dependence. They are generated by use of a built-in regression tool in the software. New parameters are then entered into the database and tested by evaluation of the prediction of equilibrium states of systems at conditions outside of those used in regression.

In this work, values for $b_{ij,0}$, $b_{ij,1}$, $c_{ij,0}$, and $c_{ij,1}$ for each solution species pair were generated separately in pure sulfate and pure chloride systems. The new parameters were then used to predict solubilities in mixed sulfate−chloride solutions that had not been used in the regression. Regression results from this work are summarized in Table 1. The MSE model has been discussed in even greater detail elsewhere.[12−15]

## Experimental Section

***Chemicals.*** Solid $MgSO_4 \cdot H_2O$ was obtained from Sigma−Aldrich at a purity level of 97 %, with the remainder as unknown impurities. To ensure that the reagent was not a more highly hydrated magnesium sulfate solid, the reagent was examined by thermogravimetric (TG) and X-ray diffraction (XRD) analysis and found to contain exclusively monohydrate. $MgCl_2 \cdot 6H_2O$ used was acquired from Fisher Scientific at reagent-grade, with a minimum purity of 99 %. HCl and $FeCl_3$ were obtained via Fisher Scientific. The HCl used was reagent-grade at a concentration between (36.5 and 38) %, and the $FeCl_3$ used was laboratory-grade.

***Apparatus.*** For these experiments, two 2 L jacketed flasks were attached in parallel with a 6 L Cole-Parmer Polystat circulating bath with a 50:50 % (by weight) ethylene glycol/water solution to ± 0.2 K of the desired temperature. Samples were removed from the reactor by use of a 50 mL syringe and filtered through Millipore 0.45 $\mu$m Millex syringe filters. In order to measure the solution densities at temperature, an oscillating U-tube densitometer was used for solutions below approximately 348 K. Above this temperature, the oscillating U-tube densitometer would not give accurate results and density was measured by taking a 1 mL aliquot of solution with a plastic-tipped autopipette and weighing it. Solution conductivities were monitored with a Foxboro 871EC electrodeless conductivity sensor.

***Procedure.*** The reaction vessel was filled to approximately 1.0 L with the solution containing all components except the one that would be at saturation and allowed to reach thermal equilibrium. An excess of the equilibrium component (either $MgCl_2 \cdot 6H_2O$ or $MgSO_4 \cdot H_2O$) was added. The conductivity was logged electronically at 1-min intervals. Once the solution conductivity had ceased to change after approximately 6 h, samples were taken with an insulated syringe that had been

**Table 1. MSE Model Interaction Parameters Developed in This Work**

| species $i$ | species $j$ | $b_{ij,0}$ | $b_{ij,1}$ | $c_{ij,0}$ | $c_{ij,1}$ |
|---|---|---|---|---|---|
| $Cl^-$ | $MgSO_{4(aq)}$ | −0.776 77 | −0.320 06 | 40.212 | 0.384 79 |
| $FeCl^{2+}$ | $Mg^{2+}$ | 85.828 | −0.036 03 | −137.23 | 0.186 74 |
| $H_3O^+$ | $Mg^{2+}$ | 192.15 | −0.768 02 | −350.84 | 1.3620 |
| $HSO_4^-$ | $Mg^{2+}$ | −426.44 | 1.364 52 | 640.11 | −2.1483 |

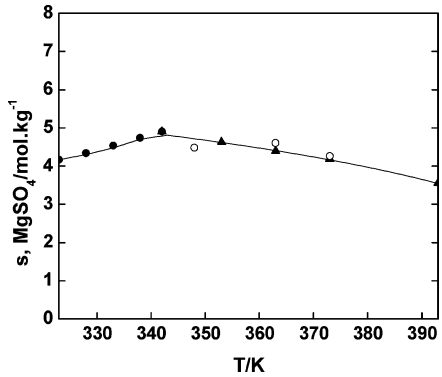


**Figure 1.** $MgSO_4$ solubility in water: ●, $MgSO_4 \cdot 6H_2O$, data from Linke and Seidell;[16] ▲, $MgSO_4 \cdot H_2O$, data from Linke and Seidell;[16] ○, $MgSO_4 \cdot H_2O$, data from this work; —, from the OLI MSE default database.

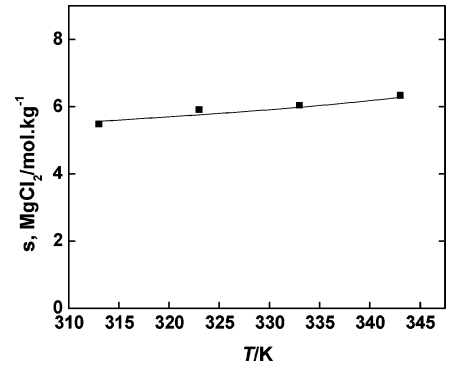


**Figure 2.** —, Regressed model, and ■, measured solubility of $MgCl_2 \cdot 6H_2O$ in 0.7 *m* $FeCl_3$ and 0.7 *m* HCl.

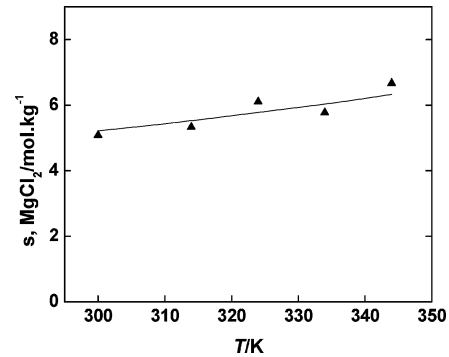


**Figure 3.** —, Regressed model, and ▲, measured solubility of $MgCl_2 \cdot 6H_2O$ in 1.0 *m* $FeCl_3$ and 0.5 *m* HCl.

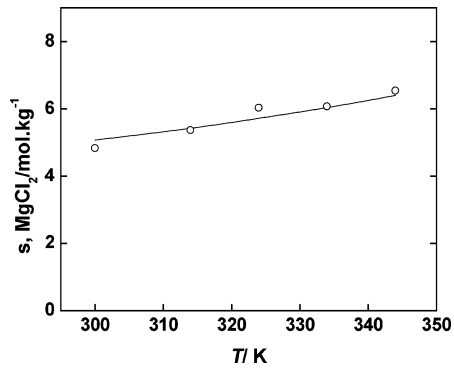


**Figure 4.** —, Regressed model, and ○, measured solubility of $MgCl_2 \cdot 6H_2O$ in 1.7 *m* $FeCl_3$ amd 0.5 *m* HCl.

preheated in an oven to experimental temperature. Solid samples taken were filtered quickly and washed immediately with acetone to ensure they would not gain structural water. Samples were then dried in a vacuum oven at 333 K overnight before being analyzed by XRD.

In tests with solids exhibiting inverse solubility trends with temperature, including tests of bischofite solubility and solubility of various magnesium sulfate hydrates in water, samples were immediately diluted to twice their initial volume with a 5 % $HNO_3$ solution. For these tests it was necessary to take density measurements at experimental temperature because as the solution cooled, salts would precipitate.

For solution samples in which all of the components remain completely dissolved at room temperature, samples were not diluted immediately after being removed from the reactor. For these tests, density measurements were taken at room temperature. All samples were diluted to concentrations below 100 $mg \cdot kg^{-1}$ Mg and analyzed by inductively coupled plasma optical emission spectroscopy (ICP-OES).

The working solubility unit for this study was moles per kilogram (molal, *m*), which is temperature-independent. For samples in which all components remain soluble at room temperature (e.g., $MgSO_4 \cdot H_2O$ in chloride solutions), densities were measured after the sample had cooled. Concentrations were measured by ICP-OES at room temperature in milligrams per liter and converted moles per kilogram by use of the room-temperature density. It was assumed that the solution-specific volumes change linearly when mixed. This assumption was shown to be valid when this dilution was performed at room temperature.

***Reproducibility.*** In order to test the validity of the experimental procedure, $MgSO_4$ solubility in pure water was measured. These results were compared with experimental data from Linke and Seidell[16] and with the OLI calculated results. It was found to match the OLI model with an average deviation of 4.0 %. Four measurements of $MgSO_4$ solubility in water were taken at 348 K; the standard deviation between replicates was 0.04 $mol \cdot kg^{-1}$ (0.9 %), and results were all within ± 0.07 $mol \cdot kg^{-1}$ (1.6 %) of the sample mean. Test results for $MgSO_4$ solubility in water are shown in Figure 1.

## Results and Discussion

***$MgCl_2/FeCl_3/HCl/H_2O$ Systems.*** For a complete model, interaction parameters between each pair of significant solution species are necessary. In order to generate MSE interaction parameters for the $FeCl^{2+}/Mg^{2+}$ species pair, $MgCl_2$ solubility data in aqueous solutions containing $FeCl_3$ and HCl were generated. $FeCl_3$ concentrations were chosen in order to simulate the acid regeneration stage of the ARNi process. HCl was added at moderate levels (≤ 0.6 $mol \cdot kg^{-1}$ HCl) to ensure that there was no precipitation of basic ferric sulfate. The system was studied at temperatures ranging from room temperature (300 K under the fume hood) to approximately 344 K. Above 344 K, it was not possible to use the sampling method described above because $MgCl_2$ salts were found to precipitate rapidly during sampling, clogging the filter.

The $FeCl_3$ and HCl concentrations do not remain precisely the same over the entire temperature range. As the reactor temperature was increased, $MgCl_2 \cdot 6H_2O$ dissolved into solution, increasing the water content and diluting dissolved electrolytes. According to Linke and Seidell,[16] in the binary $MgCl_2/H_2O$ system this effect over a temperature change from (303 to 343) K would result in an 8 % dilution. $FeCl_3$ concentrations were determined by ICP-OES and it was assumed that HCl

**Table 2. Solubility of $MgCl_2$ (1) as $MgCl_2 \cdot 6H_2O$ in Aqueous Solutions Containing HCl (2) + $FeCl_3$ (3)**

| $T$/K | $m_2$/mol·kg$^{-1}$ | $m_3$/mol·kg$^{-1}$ | $m_1$/mol·kg$^{-1}$ |
|---|---|---|---|
| 313 | 0.7 | 0.7 | 5.48 |
| 323 | 0.7 | 0.7 | 5.91 |
| 333 | 0.7 | 0.7 | 6.04 |
| 343 | 0.6 | 0.6 | 6.33 |
| 300 | 0.6 | 1.2 | 5.08 |
| 313 | 0.6 | 1.1 | 5.33 |
| 324 | 0.5 | 1.0 | 6.10 |
| 334 | 0.5 | 1.0 | 5.77 |
| 344 | 0.5 | 1.0 | 6.67 |
| 300 | 0.7 | 2.0 | 4.83 |
| 313 | 0.6 | 1.8 | 5.36 |
| 324 | 0.5 | 1.6 | 6.03 |
| 334 | 0.6 | 1.9 | 6.07 |
| 344 | 0.6 | 1.7 | 6.54 |

concentrations changed proportionally. Regression results are shown in Figures 2 to 4, and experimental results are reported in Table 2.

Over the entire temperature range studied, the equilibrium solid was confirmed, via XRD analysis, to be $MgCl_2 \cdot 6H_2O$. This is consistent with studies of the $MgCl_2/H_2O$ system over the temperature range of (270 to 389) K, a much wider range than that being tested in this study.[16−18]

Also, at all conditions examined, $MgCl_2 \cdot 6H_2O$ solubility is directly proportional to temperature. This is the same trend seen in literature solubility results for the binary $MgCl_2/H_2O$ system[16−18] and the ternary $MgCl_2/HCl/H_2O$ system,[19] although in the $MgCl_2/FeCl_3/HCl/H_2O$ system, $MgCl_2 \cdot 6H_2O$ solubilities are slightly lower at constant temperatures or acid levels. $FeCl_3$ addition increases the chloride content of the system, and the solubility of $MgCl_2 \cdot 6H_2O$ is reduced by the common ion effect with chloride. OLI model results were fitted to the solubility data in these systems with an average absolute deviation of 0.15 mol·kg$^{-1}$ and an average absolute relative deviation of 2.6 %.

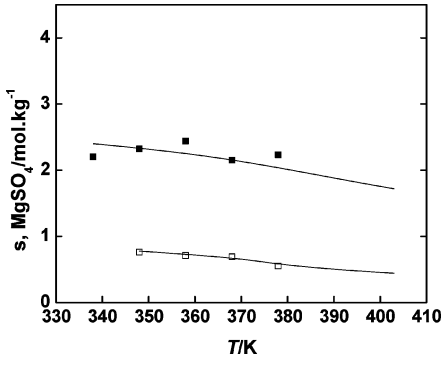


**Figure 5.** Line, predicted model, and squares, measured solubility of $MgSO_4 \cdot H_2O$ in high-strength chloride solutions: ■, 1.0 *m* $FeCl_3$/2.3 *m* HCl/1.0 *m* $MgCl_2$; □, 1.0 *m* $FeCl_3$/1.0 *m* HCl/3.5 *m* $MgCl_2$.

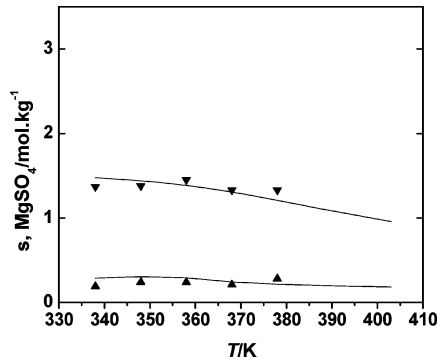


**Figure 6.** Line, predicted model, and triangles, measured solubility of $MgSO_4 \cdot H_2O$ in high-strength chloride solutions: ▼, 1.0 *m* $FeCl_3$/1.6 *m* HCl/2.3 *m* $MgCl_2$; ▲, 1.0 *m* $FeCl_3$/0.5 *m* HCl/4.8 *m* $MgCl_2$.

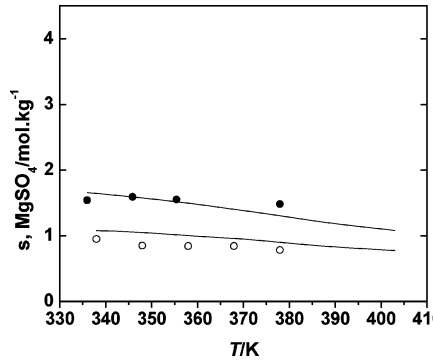


**Figure 7.** Lines, predicted model, and circles, measured solubility of $MgSO_4 \cdot H_2O$ in high-strength chloride solutions: ●, 1.0 *m* $FeCl_3$/2.3 *m* HCl/2.3 *m* $MgCl_2$; ○, 1.0 *m* $FeCl_3$/2.3 *m* HCl/3.5 *m* $MgCl_2$.

**Table 3. Solubility of $MgSO_4$ (1) as $MgSO_4 \cdot H_2O$ in Aqueous Solutions Containing HCl (2) + $FeCl_3$ (3) + $MgCl_2$ (4)**

| $T$/K | $m_2$/mol·kg$^{-1}$ | $m_3$/mol·kg$^{-1}$ | $m_4$/mol·kg$^{-1}$ | $m_1$/mol·kg$^{-1}$ |
|---|---|---|---|---|
| 336 | 2.3 | 1.0 | 2.3 | 1.54 |
| 347 | 2.3 | 1.0 | 2.3 | 1.59 |
| 356 | 2.3 | 1.0 | 2.3 | 1.55 |
| 378 | 2.3 | 1.0 | 2.3 | 1.48 |
| 338 | 2.3 | 1.0 | 1.0 | 2.20 |
| 348 | 2.3 | 1.0 | 1.0 | 2.32 |
| 358 | 2.3 | 1.0 | 1.0 | 2.44 |
| 368 | 2.3 | 1.0 | 1.0 | 2.15 |
| 378 | 2.3 | 1.0 | 1.0 | 2.23 |
| 338 | 1.6 | 1.0 | 2.3 | 1.37 |
| 348 | 1.6 | 1.0 | 2.3 | 1.38 |
| 358 | 1.6 | 1.0 | 2.3 | 1.45 |
| 368 | 1.6 | 1.0 | 2.3 | 1.33 |
| 378 | 1.6 | 1.0 | 2.3 | 1.33 |
| 338 | 2.3 | 1.0 | 3.5 | 0.95 |
| 348 | 2.3 | 1.0 | 3.5 | 0.85 |
| 358 | 2.3 | 1.0 | 3.5 | 0.84 |
| 368 | 2.3 | 1.0 | 3.5 | 0.81 |
| 378 | 2.3 | 1.0 | 3.5 | 0.78 |
| 348 | 1.0 | 1.0 | 3.5 | 0.76 |
| 358 | 1.0 | 1.0 | 3.5 | 0.71 |
| 368 | 1.0 | 1.0 | 3.5 | 0.65 |
| 378 | 1.0 | 1.0 | 3.5 | 0.56 |
| 338 | 0.5 | 1.0 | 4.8 | 0.19 |
| 348 | 0.5 | 1.0 | 4.8 | 0.24 |
| 358 | 0.5 | 1.0 | 4.8 | 0.24 |
| 368 | 0.5 | 1.0 | 4.8 | 0.21 |
| 378 | 0.5 | 1.0 | 4.8 | 0.28 |

***$MgSO_4/MgCl_2/FeCl_3/HCl/H_2O$ Systems.*** To test the predictability of the model, experimental data were generated in aqueous solutions containing $FeCl_3$, $MgCl_2$, and HCl, the main components of the inlet stream to the acid regeneration stage of the ARNi process. At all test conditions, the expected equilibrium solid is $MgSO_4 \cdot H_2O$, which is the desired phase for magnesium rejection. Confirmatory XRD analysis was performed on the solids from the sample taken at the lowest temperature at each set of electrolyte concentrations. In all cases, it was indeed confirmed that $MgSO_4 \cdot H_2O$ was the equilibrium phase. From Linke and Seidell,[16] the phase stability region of $MgSO_4 \cdot H_2O$ in water extends to at least 513 K, and from Marshall et al.,[20] the phase stability of $MgSO_4 \cdot H_2O$ in $H_2SO_4$ solutions at concentrations between (0 and 1.5) mol·kg$^{-1}$ extends to at least 573 K, much higher than the maximum temperature of these tests. Thus, it was accepted that the solid

did not change from $MgSO_4 \cdot H_2O$ as the temperature was increased from (338 to 378) K. Experimental and model-predicted solubility values are shown in Figures 5 to 7. Experimental results are summarized in Table 3.

By examining Figures 5 to 7 we can identify some $MgSO_4 \cdot H_2O$ solubility trends. In all cases, the change in temperature has a minimal effect. In contrast, the $MgCl_2$ concentration has a more pronounced effect. This is expected because of the common ion effect.

The effect of HCl level is seen by comparing Figures 5 and 7, particularly the data sets that have the same $MgCl_2$ and $FeCl_3$ concentrations but different HCl levels. We can see that HCl has a moderate positive effect on $MgSO_4 \cdot H_2O$ solubility. Kieserite is a neutral salt and the hydronium ion is not directly involved in its dissolution process. Nevertheless, bisulfate formation in the presence of acid increases the capacity of the solution to dissolve $MgSO_4$. Regression results from this work are summarized in Table 1.

## Conclusions

In this work, $MgCl_2 \cdot 6H_2O$ solubility in solutions containing $FeCl_3$, HCl, and $H_2O$ was measured. These data were then used to calibrate a thermodynamic model with the goal of modeling the solubility of $MgSO_4 \cdot H_2O$ under conditions similar to those of the acid regeneration stage of the ARNi process. In order to test the validity of the model, $MgSO_4 \cdot H_2O$ solubility was measured in solutions containing (1.0 to 4.8) $mol \cdot kg^{-1}$ $MgCl_2$, (0.5 to 2.3) $mol \cdot kg^{-1}$ HCl, and 1.0 $mol \cdot kg^{-1}$ $FeCl_3$ from (336 to 378) K and compared with model predictions. Experimental measurements were found to match model-calculated solubility values with an average absolute deviation of $\pm$ 0.09 $mol \cdot kg^{-1}$ and an average absolute relative deviation of 11.1 %.

The development of a model capable of predicting $MgSO_4 \cdot H_2O$ solubility in systems containing $FeCl_3$, HCl, $MgCl_2$, and $H_2O$ can give process developers insight into the behavior of this system and facilitate process design and development.

### Acknowledgment

We acknowledge the support of Anglo American plc and OLI Systems, Inc.

## Literature Cited

(1) McDonald, R. G.; Whittington, B. Atmospheric acid leaching of nickel laterites review. Part I. Sulphuric acid technologies. *Hydrometallurgy* **2008a**, *91*, 35–55.
(2) McDonald, R. G.; Whittington, B. Atmospheric acid leaching of nickel laterites review. Part II. Chloride and bio-technologies. *Hydrometallurgy* **2008b**, *91*, 56–69.
(3) Georgiou, D.; Papangelakis, V. G. Sulphuric acid pressure leaching of a limonitic laterite: chemistry and kinetics. *Hydrometallurgy* **1998**, *49*, 23–46.
(4) Francis, B. R.; Reid, J. G.; Barnett, S. Process for Nickel and Cobalt Extraction from Laterite Ores. International Patent WO 2004/067787 A1, July 12, 2004.
(5) Hunter, W. L.; Danton, L.; Stickney, W. A. Smelting of Nickel Oxide Ores to Produce Ferronickel. United States Patent 3854936, December 12, 1974.
(6) Smit, J. T.; Steyl, J. D. T. Leaching Process in the Presence of Hydrochloric Acid for the Recovery of a Value Metal from an Ore. International Patent WO 2007/074360 A2, July 5, 2007.
(7) Steyl, J. D. T.; Pelser, M.; Smit, J. T. *Atmospheric Chloride Leach for Nickel Laterite Ores. In Robert S. Shoemaker International Symposium on Hydrometallurgy 2008*; Young, C., et al., Eds.; SME: Littleton, 2008.
(8) Papangelakis, V. G.; Liu, H.; Rubisov, D. *2004. Solution chemistry and reactor modelling of the pal process: successes and challenges. In International Laterite Nickel Symposium - 2004*; Imrie, W. P., Lane, D. M., Eds.; The Minerals, Metals and Materials Society: Charlotte, 2004.
(9) Harris, G. B.; Magee, T. J.; Lakshmanan, V. I. *The Jaguar Nickel Inc. Sechol Laterite Project Atmospheric Chloride Leach Processs. In International Laterite Nickel Symposium - 2004*; Imrie, W. P., Lane, D. M., Eds.; The Minerals, Metals and Materials Society: Charlotte, 2004.
(10) Jones, M. W.; Papangelakis, V. G.; Steyl, J. D. T. *Chemical Modelling of MgSO4 Solubility in Atmospheric Chloride Leaching of Laterites. In Robert S. Shoemaker International Symposium on Hydrometallurgy 2008*; Young, C., et al., Eds.; SME: Littleton, 2008.
(11) Tanger, J. C.; Helgeson, H. C. Calculation of the Thermodynamic and Transport Properties of Aqueous Species at High Pressures and Temperatures: Revised Equations of State for the Standard Partial Molal Properties of Ions and Electrolytes. *Am. J. Sci.* **1988**, *288*, 19–98.
(12) Wang, P.; Anderko, A.; Young, R. A speciation-based model for mixed-solvent electrolyte systems. *Fluid Phase Equilib.* **2002**, *203*, 141–176.
(13) Wang, P.; Springer, R; Anderko, A.; Young, R. 2004. Modeling phase equilibria and speciation in mixed-solvent electrolyte systems. *Fluid Phase Equilib.* **2004**, *222*−*223*, 11–17.
(14) Wang, P.; Anderko, A.; Springer, R.; Young, R. Modeling phase equilibria and speciation in mixed-solvent electrolyte systems: II. Liquid-liquid equilibria and properties of associating electrolyte solutions. *J. Mol. Liq.* **2006**, *125*, 37–44.
(15) Azimi, G.; Papangelakis, V. G.; Dutrizac, J. E. Modelling of calcium sulphate solubility in concentrated multi-component sulphate solutions. *Fluid Phase Equilib.* **2007**, *260*, 300–315.
(16) Linke, W. F.; Seidell, A. *1958. Solubilities, Inorganic and Metal-Organic Compounds.*; D.Van Nostrand Company, Inc.: Princeton, N.J., 1958.
(17) Clynne, M. A.; Potter, R. Solubility of Some Alkali and Alkaline Earth Chlorides in Water at Moderate Temperatures. *J. Chem. Eng. Data* **1979**, *24* (4), 338–340.
(18) Prutton, C.; Tower, O. The System Calcium Chloride - Magnesium Chloride - Water at 0,−15 and−30 C. *J. Am. Chem. Soc.* **1932**, *54* (8), 3040–3047.
(19) Dähne, C. Bestimung der Loslichkeitsisothermen des Systems HCl-$MgCl_2$-$H_2O$ zwischen−55 und 80 °C. *Z. Anorg. Allg. Chem.* **1969**, *371*, 59–73.
(20) Marshall, W. L.; Slusher, R.; Smith, F. 1965. Aqueous Systems at High Temperature. XVSolubility and Hydrolytic Instability of Magnesium Sulfate in Sulfuric Acid-Water and Deuterosulfuric Acid-Deuterium Oxide Solutions, 200 to 350 °C. *J. Chem. Eng. Data* **1965**, *10* (4), 353–358.

Received for review October 7, 2008. Accepted March 27, 2009. The authors gratefully acknowledge the funding provided by Anglo American plc and the Ontario Graduate Scholarship in Science and Technology.

JE800735H